

AD-A110 819

DOUGLAS AIRCRAFT CO. LONG BEACH CA

F/G 20/4

AN IMPROVED HIGHER ORDER PANEL METHOD FOR THREE-DIMENSIONAL LIF--ETC(U)

DEC 81 J L HESS, D M FRIEDMAN

N62269-80-C-0228

UNCLASSIFIED

MDC-J2162

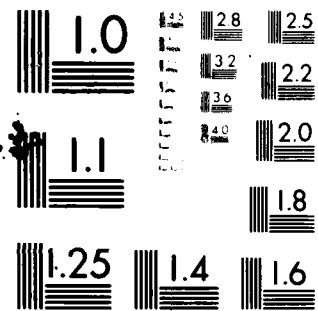
NADC-79277-60

NL

1.1
A
2.10015



END
DATE
FILMED
3 82
DTIC



MICROCOPY RESOLUTION TEST CHART
NATIONAL BUREAU OF STANDARDS-1963-A

REPORT NO. NADC-79277-60

REPORT NO. MDC J21E2



12

LEVEL II

AD A110819

AN IMPROVED HIGHER ORDER PANEL METHOD FOR THREE-DIMENSIONAL
LIFTING POTENTIAL FLOW

John L. Hess and Douglas M. Friedman
Aerodynamics Research
Douglas Aircraft Company
3855 Lakewood Boulevard
Long Beach, California 90846

DECEMBER 1981

DTIC
ELECTED
FEB 11 1982
B

FINAL REPORT

AIRTASK No. A320320D/001A/1R023-02-000

APPROVED FOR PUBLIC RELEASE; DISTRIBUTION UNLIMITED

DTIC FILE COPY

Prepared for
NAVAL AIR DEVELOPMENT CENTER
Warminster, Pennsylvania 18974

8 2 0 2 1 13

REPORT NO. NADC-79277-60

REPORT NO. MDC J2162



AN IMPROVED HIGHER ORDER PANEL METHOD FOR THREE-DIMENSIONAL
LIFTING POTENTIAL FLOW

John L. Hess and Douglas M. Friedman
Aerodynamics Research
Douglas Aircraft Company
3855 Lakewood Boulevard
Long Beach, California 90846

DECEMBER 1981

FINAL REPORT

AIRTASK No. A3203200/001A/1R023-02-000

APPROVED FOR PUBLIC RELEASE; DISTRIBUTION UNLIMITED

Prepared for
NAVAL AIR DEVELOPMENT CENTER
Warminster, Pennsylvania 18974

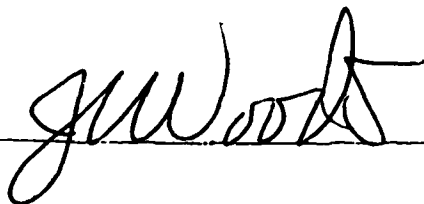
NOTICES

REPORT NUMBERING SYSTEM - The numbering of technical project reports issued by the Naval Air Development Center is arranged for specific identification purposes. Each number consists of the Center acronym, the calendar year in which the number was assigned, the sequence number of the report within the specific calendar year, and the official 2-digit correspondence code of the Command Office or the Functional Directorate responsible for the report. For example: Report No. NADC-76015-20 indicates the fifteenth Center report for the year 1976, and prepared by the Systems Directorate. The numerical codes are as follows:

CODE	OFFICE OR DIRECTORATE
00	Commander, Naval Air Development Center
01	Technical Director, Naval Air Development Center
02	Comptroller
10	Directorate Command Projects
20	Systems Directorate
30	Sensors & Avionics Technology Directorate
40	Communication & Navigation Technology Directorate
50	Software Computer Directorate
60	Aircraft & Crew Systems Technology Directorate
70	Manning Assessment Resources
80	Engineering Support Group

PRODUCT ENDORSEMENT - The discussion or instructions concerning commercial products herein do not constitute an endorsement by the Government nor do they convey or imply the license or right to use such products.

APPROVED BY:



DATE:

11/2/81

Enclosure (4)

1.0 ABSTRACT

A previous report described a higher-order three-dimensional panel method that represents the body about which flow is to be computed by means of curved four-sided surface panels having linearly varying source and vorticity distributions. The method of accounting for lift was incomplete, and the main purpose of the present work was to remedy this defect. A number of other modifications to the method were also made to improve its efficiency and accuracy.

The modifications documented here are: formulas for the edge-vortex influences, which previously had been neglected; new surface vorticity formulas that express its influences in terms of source influences; a modified global vorticity algorithm to improve continuity over the surface, and, an extrapolated Kutta condition.

[illegible]

2.0 TABLE OF CONTENTS

	<u>Page</u>
1.0 Abstract	1
2.0 Table of Contents	2
3.0 Principal Notation	3
4.0 Introduction	5
5.0 Calculation of Vorticity Induced Velocities in Terms of Source Induced Velocities	8
5.1 Background.	8
5.2 General Theory	8
5.3 Calculation of the Velocity Induced by a Panel	9
5.4 Assembly of the Vorticity Formulas	12
6.0 The Line Vortex Along a Streamwise Edge of a Panel	14
6.1 Background	14
6.2 Derivation of the Influence of an Edge Vortex	14
6.3 Formulas for the Edge-Vortex Influence	16
6.4 Far-Field Formulas	18
7.0 Modification of the Global Vorticity Algorithm	20
7.1 Considerations of Continuity and Accuracy	20
7.2 Modification of the Chordwise Vorticity on a Panel	21
7.3 Modification of the Spanwise Fitting Procedure	22
8.0 The Use of an Extrapolated Kutta Condition	23
9.0 Calculated Examples	24
10.0 References	33
Appendix A. A Surface Geometry Fitting Procedure Based on Bicubic Splines	34

3.0 PRINCIPAL NOTATION

A	area of the flat projected panel (Figure 1)
B	derivative of the equivalent dipole strength along an N-line
c	constant governing the equivalent dipole term quadratic in η
F,S	used as subscripts to denote quantities associated with the first and second N-lines of a panel, respectively
h	arc length along an N-line from the trailing edge to the η -axis of panel coordinates
$\hat{i}_e, \hat{j}_e, \hat{k}_e$	unit vectors along the axes of the panel coordinate system
J_{mn}	functions defined by equations (6.3.1), (6.3.2) and (6.3.4)
L(total)	total arc length of an N-line from lower surface trailing edge to upper surface trailing edge
P,Q,R	panel "curvatures," i.e., second derivatives of the shape of the curved panel at the origin of panel coordinates
r	magnitude of \vec{r}
\vec{r}	vector from a point on the curved panel to a point in space where velocity is to be evaluated
\vec{r}_f	vector from a point on the projected flat panel to a point in space where velocity is to be evaluated
S	surface area of the curved panel (Figure 1)
T	slope of an N-line, eq. (6.2.3)
\vec{V}	velocity vector
u,v	parameters in the parametric cubic fit
w	width of a panel between N-lines
x,y,z	coordinates of a point in space where velocity is to be evaluated
ζ_2	quadratic surface approximating the curved panel, eq. (5.3.2)
η_1, η_3	coordinates of the first and second N-lines, respectively, in panel coordinates
μ	equivalent dipole strength. When used with subscripts x and y it denotes the corresponding derivative of μ at the origin of panel coordinates

ξ, η, ζ	coordinates of a point on the curved panel in panel coordinates. Setting $\zeta = 0$ gives the corresponding point on the projected flat panel
σ	source density
$\vec{\omega}$	vorticity vector, used with various subscripts

4.0 INTRODUCTION

Reference 1 describes a so-called first-order panel method for calculating potential flow about arbitrary three-dimensional lifting bodies. The program deck corresponding to this method has been distributed widely and indeed has become a standard design tool for subsonic aerodynamic analysis throughout the country. Recently a higher-order version of the panel method was constructed as described in reference 2. Compared to the first-order method of reference 1, the higher-order method achieves greater calculational accuracy for a given panel number and thus has the potential to reduce cost substantially for a given accuracy and to calculate flow about more complicated configurations. The initial nonlifting version of the higher-order method, which was documented in reference 3, has already been used in design applications, for example reference 4. However, complete formulas and logical procedures for the method were first presented in reference 2, which also included provisions for lifting effects. The lifting method described in reference 2 to a large extent has the nature of a pilot method for proving the approach, rather than a final general procedure.

The work described in this report consists of modifications to the method of reference 2 that greatly increase its accuracy and numerical efficiency. To make the present document self-contained would require a complete description of the higher-order panel method and thus a duplication of large portions of reference 2. Since reference 2 is generally available, the consequent large increase in the length of the present report seems neither necessary nor desirable. Accordingly, reference 2 is relied upon to provide the general ideas and philosophy of the higher-order method, as well as detailed formulas and logic. Indeed references will frequently be made to sections and even individual equations of reference 2. A few features of the higher-order method that bear directly on the modifications described in this report are mentioned below. But the intention is one of emphasis not of completeness.

A panel method discretizes the body about which flow is to be computed, representing it by a large number of small four-sided surface panels, on each of which are distributions of source and dipole or vorticity. A control point is selected on each panel where the normal-velocity boundary condition

is enforced and where flow quantities are eventually calculated. In lifting cases a Kutta condition is applied to insure smooth flow off wing trailing edges. In essence the source strengths on the panels are adjusted to satisfy the normal-velocity boundary conditions, and thus each panel has an independent value of source strength. The variation of dipole or vorticity strength over the surface is fitted by certain global algorithms to obtain expressions containing a number of adjustable parameters equal to the number of locations where the Kutta condition is applied.

The key calculational unit in a panel method is the set of formulas giving the velocities induced at a point in space by the source and dipole or vorticity distributions on a panel. In the first-order method of reference 1 the panels are planar and the required induced velocities due to constant source and quadratic dipole distributions may be obtained exactly by means of analytic integration over the panel. When the point in question is far from the panel, approximate "far-field" formulas are used to reduce computing time. In the higher-order method of reference 2, the panels are conceptually curved. Since analytic integration over a curved panel is not possible, the induced velocities due to linearly varying source and vorticity distributions on the curved panel are expressed as expansions about the effects of the flat panel that is the projection of the curved panel in the tangent plane. Integration over the "projected flat panel" of the various terms in the expansion can be performed analytically. The validity and consistency of the expansions are discussed in reference 2. Approximate expressions for the terms of the expansion are used at distant points. The errors due to using these far-field expressions are independent of and can be made small with respect to the truncation error of the expansion about the projected flat panel.

The analytic expressions in reference 2 for the effects of panel vorticity are extremely cumbersome. Moreover, they do not lend themselves to efficient far-field approximations. The result is long computing times for the method as presented in reference 2. This situation has been remedied by relating the vorticity-induced velocities to the source-induced velocities and thus obtaining the former in essentially no additional time. The far-field problem no longer arises because the source far-field approximation is all that is required. This modification is discussed in section 5.0.

As discussed in reference 2, vorticity has been employed on a panel rather than a dipole distribution because it leads to a simpler expansion about the projected flat panel. Thus the effects of line vortices around the perimeter of the panel are neglected. Over the portions of the surface away from any physical edges the effect of the line vortex along each edge of a panel is cancelled, at least to some order, by that of the line vortex along the edge of the adjacent panel. The result is a relatively weak line vortex. At physical edges of the body, e.g., a wing tip, there can be no such cancellation, and indeed a strong edge or tip vortex is known to be present. It turns out that it is the trailing edge vortices that are important. Section 6.0 presents formulas that account for the effects of such edge vortices.

So-called global vorticity algorithms are used to relate the vorticity strengths on the panels and thus reduce the variation of vorticity over the surface to analytic expressions depending on a number of parameters equal to the number of locations at which the Kutta condition is prescribed. Section 7.0 describes two improvements to the global vorticity algorithms of reference 2. One is concerned with minimizing spanwise vortices at interior panel edges (previous paragraph) and the other with an improvement in the spanwise vorticity fit that eliminates extraneous wake vorticity.

The Kutta condition used in all versions of the panel method is an equal-pressure condition applied at the upper and lower trailing edge of a wing. In references 1 and 2 the pressures set equal are those at the upper and lower control points nearest the trailing edge for each spanwise location. Thus the equal-pressure condition is applied at a distance of half a panel length from the trailing edge. This is an acceptable approximation for a first-order method, but it penalizes a higher-order method unnecessarily. Section 8.0 describes an improved Kutta condition that extrapolates upper and lower surface pressures to the trailing edge before setting them equal.

Finally, the geometric procedure described in reference 2 for calculating panel curvatures, control points, and normal vectors has been found to be unsatisfactory (in some cases). Accordingly, it has been replaced by a more elaborate procedure. Although this modification is outside the scope of the work reported here, it seemed that for completeness a description of it should be included. Thus it is presented in Appendix A.

5.0 CALCULATION OF VORTICITY INDUCED VELOCITIES IN TERMS OF SOURCE INDUCED VELOCITIES

5.1 Background

As has been mentioned, the expressions for induced velocity due to any polynomial distribution of singularity can be analytically integrated over a flat panel. Moreover, the only transcendental functions that occur are the logarithms and inverse tangents that are already present in the first-order constant-source formulas. Thus, the expressions for higher-order effects, which are obtained by integration over the projected flat panel, can, at least potentially, be evaluated in computing times only modestly larger than those for the first-order formulas. This was certainly true for the two-dimensional higher-order method of reference 5 and to a lesser extent for the nonlifting version of the present method (reference 3). However, there are limits to the insensitivity of computing time. The formulas for the vorticity effects that are presented in section 6.3 of reference 2 are so elaborate that they add substantially to the required computing time. Most of the complications arise from the curvature-dependent terms. Moreover, these formulas are not suitable for efficient far-field approximation. Thus the 90% or so of the velocity influences that are calculated by far-field formulas require considerably more computing time for the vorticity effects than for the source effects, the latter of which do have efficient far-field approximations.

5.2 General Theory

The calculation of the vorticity influences can be made much more efficient by expressing them in terms of the corresponding source influences, which of course must be calculated in any event. The use of this procedure was put forward in reference 6. The portion of the theory that is needed for the present purpose is quite easy to state.

Suppose there is a variable source density σ on a portion of a plane or curved surface S . The velocity due to this at a point (x,y,z) is

$$\vec{V}(\text{source}) = \iint_S \frac{\vec{r}}{r^3} \sigma dS \quad (5.2.1)$$

where (x_q, y_q, z_q) is a point on s and where

$$\vec{r} = (x - x_q)\vec{i} + (y - y_q)\vec{j} + (z - z_q)\vec{k} \quad (5.2.2)$$

As usual r is the magnitude of \vec{r} (see Figure 1). If there is a vorticity distribution of S of strength

$$\vec{\omega} = \omega \vec{e} \quad (5.2.3)$$

the Biot-Savart law gives the resulting induced velocity as

$$\vec{V}(\text{vorticity}) = \iint_S \frac{\vec{e} \times \vec{r}}{r^3} \omega dS \quad (5.2.4)$$

Then if \vec{e} is a constant vector and if ω has the same spatial variation as σ , the velocity due to the vorticity distribution may be expressed in terms of the velocity due to the source distribution as

$$\vec{V}(\text{vorticity}) = \vec{e} \times \vec{V}(\text{source}) \quad (5.2.5)$$

since $\vec{\omega}$ can be resolved into components, each of which has a constant direction, the restriction to a constant \vec{e} is not serious. Although the above results apply to a curved surface S , it is far simpler to apply to a flat surface. In the present context the above is applied to the flat projected panel.

5.3 Calculation of the Velocity Induced by a Panel

Figure 1 illustrates the projection of a curved panel S on the surface to a flat panel A in the tangent plane. In particular, Figure 1 illustrates \vec{r} as given in (5.2.2) above and the vector \vec{r}_f from a point of the projected flat panel to the point (x, y, z)

$$\vec{r}_f = (x - \xi)\vec{i}_e + (y - \eta)\vec{j}_e + z\vec{k}_e \quad (5.3.1)$$

where $\vec{i}_e, \vec{j}_e, \vec{k}_e$ are unit vectors along the axes of the panel coordinate system. The vertical distance z between the curved panel and its projection is approximated by its leading term z_2 , which represents a surface of second degree

$$\zeta_2 = P\xi^2 + 2Q\xi\eta + R\eta^2 \quad (5.3.2)$$

where P, Q, R are the second derivatives of ζ at the origin of panel coordinates — the so-called surface curvatures.

The aim is to parallel the development of section 5.3 of reference 2 and express the results in terms of source effects. From equation (53) of reference 2 it is seen that a two-term expansion of the vector vorticity distribution is

$$\vec{\omega} = \vec{\omega}_0 + \vec{\omega}_1 \quad (5.3.3)$$

where

$$\vec{\omega}_0 = \mu_y \vec{i}_e - \mu_x \vec{j}_e \quad (5.3.4)$$

is zero order and

$$\begin{aligned} \vec{\omega}_1 = & 2(\mu_{xy}\xi + \mu_{yy}\eta)\vec{i}_e - 2(\mu_{xx}\xi + \mu_{xy}\eta)\vec{j}_e + \\ & + 2[-(Q\xi + R\eta)\mu_x + (P\xi + Q\eta)\mu_y]\vec{k}_e \end{aligned} \quad (5.3.5)$$

is first order. The constants μ_x, μ_{xx} , etc. are the derivatives of the equivalent dipole distribution as given by equation (50) of reference 2. From (5.3.1) and (5.2.2) expressed in panel coordinates:

$$\vec{r} = \vec{r}_f - \zeta_2 \vec{k}_e \quad (5.3.6)$$

Thus a two-term expansion of the velocity at (x, y, z) due to the vorticity on the panel is

$$\vec{V}_\omega = \iint_S \frac{\vec{\omega} \times \vec{r}}{r^3} dS = \iint_A \left\{ \frac{\vec{\omega}_0 \times \vec{r}_f}{r_f^3} \left(1 + 3z \frac{\zeta_2}{r_f^2} \right) + \frac{\vec{\omega}_1 \times \vec{r}_f}{r_f^3} - \zeta_2 \frac{\vec{\omega}_0 \times \vec{k}_e}{r_f^3} \right\} dA \quad (5.3.7)$$

$$= \vec{\omega}_0 \times \iint_A \left[\frac{\vec{r}_f}{r_f^3} \left(1 + 3z \frac{\zeta_2}{r_f^2} \right) - \zeta_2 \frac{\vec{k}_e}{r_f^3} \right] dA + \iint_A \frac{\vec{\omega}_1 \times \vec{r}_f}{r_f^3} dA \quad (5.3.8)$$

By taking the gradient of the $\phi^{(0)}$ and $\phi^{(c)}$ terms of the source expansion on page 20 of reference 2, it can be seen that the integral multiplying

$\vec{\omega}_0$ above is just the sum of superscript 0 and c source terms for unit source density. Specifically this combination is the velocity

$$\vec{V}' = \vec{V}^{(0)} + [P\vec{V}^{(P)} + 2Q\vec{V}^{(Q)} + R\vec{V}^{(R)}] \quad (5.3.9)$$

where the quantities on the right of (5.3.9) are as defined in section 6.2 of reference 2, and the combined velocity \vec{V}' is explicitly calculated by the existing code.

To analyze the remaining term of (5.3.8), collect terms in equation (5.3.5) to obtain

$$\vec{\omega}_1 = 2(\xi\vec{q}_x + \eta\vec{q}_y) \quad (5.3.10)$$

where the vectors

$$\begin{aligned} \vec{q}_x &= \mu_{xy}\vec{i}_e - \mu_{xx}\vec{j}_e + (P\mu_y - Q\mu_x)\vec{k}_e \\ \vec{q}_y &= \mu_{yy}\vec{i}_e - \mu_{xy}\vec{j}_e + (Q\mu_y - R\mu_x)\vec{k}_e \end{aligned} \quad (5.3.11)$$

are constants in the integration. The integrals that result from using (5.3.10) in the second term of (5.3.8) are the velocities due to linearly varying source densities in the ξ and η directions having unit slope, i.e. $\vec{V}^{(1x)}$ and $\vec{V}^{(1y)}$ from section 6.2 of reference 2.

Thus the velocity (5.3.7) due to vorticity on the panel may be expressed in terms of source velocities as follows

$$\vec{V}_\omega = \vec{\omega}_0 \times \vec{V}' + 2[\vec{q}_x \times \vec{V}^{(1x)} + \vec{q}_y \times \vec{V}^{(1y)}] \quad (5.3.12)$$

It is interesting to note that (5.3.12) can be evaluated directly in reference coordinates after the relevant source velocities have been calculated and put into this system. As regards the velocities due to the vorticity, this not only means that no transformations between panel and reference coordinates are required, but it also means that the question of far-field calculation need never arise. If the source velocities have been computed by far-field

formulas, they simply are used in (5.3.12), so that in effect the vorticity calculation uses the source far-field procedure. The present code takes advantage of the second of these facts, the use of far-field source formulas, but performs the calculation in panel coordinates.

Formulas (5.3.4), (5.3.11) and (5.3.12) replace the elaborate formulas of section 6.3 of reference 2.

5.4 Assembly of the Vorticity Formulas

The formulas of section 5.3 give the difficult portion of the vorticity calculation. However, the task remains to collect the terms of the vorticity-induced velocity into velocities associated with the first and second N-lines of the panel in a manner similar to that of section 9.0 of reference 2. Basically this is a matter of performing the indicated vector cross products of section 5.3 above and using formulas (141) of reference 2 for the μ derivatives. This last is most easily done computationally by means of the following logical table

μ -derivative	First N-line	Second N-line	
μ_x	$\frac{\eta_1}{w}$	$-\frac{\eta_3}{w}$	
μ_y	$\frac{h_F}{w} - c(\eta_1 + \eta_3)$	$-\frac{h_S}{w} + c(\eta_1 + \eta_3)$	
μ_{xx}	d	$-d$	(5.4.1)
μ_{xy}	$\frac{1}{2w}$	$-\frac{1}{2w}$	
μ_{yy}	c	$-c$	

where all quantities have the same meaning as in reference 2 section 9.2. The foregoing are on-body formulas. For wake panels set

$$\mu_x = \mu_{xx} = \mu_{xy} = 0 \quad (5.4.2)$$

$$h_F = L_F \text{ (total)}, \quad h_S = L_S \text{ (total)}$$

In performing the indicated cross products it will be recalled that the components of \vec{i}_e , \vec{j}_e , \vec{k}_e ($\vec{k}_e = \vec{n}$) in reference coordinates are the entries of the panel's transformation matrix a_{mn} , i.e.

$$\begin{aligned}\vec{i}_e &= a_{11}\vec{i} + a_{12}\vec{j} + a_{13}\vec{k} \\ \vec{j}_e &= a_{21}\vec{i} + a_{22}\vec{j} + a_{23}\vec{k} \\ \vec{k}_e &= a_{31}\vec{i} + a_{32}\vec{j} + a_{33}\vec{k}\end{aligned}\tag{5.4.3}$$

If the calculation is performed in panel coordinates, e.g. the near field, these are simply the unit vectors along the coordinate axes, and, for example the coefficient of \vec{i}_e is simply V_x in the panel coordinates.

The formulas of section 5.3 above and the present section permit determination of the F and S vorticity influences in the form of equation (143) of reference 2 in a straightforward way.

6.0 THE LINE VORTEX ALONG A STREAMWISE EDGE OF A PANEL

6.1 Background

As mentioned in the Introduction and discussed in section 5.3 of reference 2, the use of a vorticity distribution on a panel rather than a dipole distribution means that the effects of a line vortex around the perimeter of the panel are neglected. Away from a physical edge of the body this neglect might be justified because line vortices on the edges of adjacent panels tend to cancel. It turns out this is true for spanwise panel edges but not for streamwise edges. That is, the edge-vortex contribution to the bound vorticity has been found to be relatively unimportant but the trailing edge vorticity along the N-lines must be accounted for. This matter is discussed more in section 7.0 and examples are given in section 8.0. At a wing tip or other physical edge of a lifting body there is a strong edge vortex whose neglect renders the solution significantly nonpotential. The absence of machinery for calculating the effects of such an edge vortex restricts the method of reference 2 to very specialized lifting configurations. The analysis of this section removes this restriction. The same formulas are used for interior edge vortices along the N-lines.

There are several ways of accounting for the effect of the edge vortex, all of which are theoretically equivalent to some order of accuracy. The approach used here is the analogy of that used throughout the higher-order development. A vortex lying along the edge of the curved panel is projected into the tangent plane.

6.2 Derivation of the Influence of an Edge Vortex

The equation of the curved panel is (5.3.2). For definiteness consider the case when the edge in question lies in the plane $\eta = \eta_1$, i.e. the first N-line. The modifications for the case of the second N-line are obvious. Thus the curve c along which the vortex lies is

$$\zeta = \zeta(\xi) = P\xi^2 + 2Q\xi\eta_1 + R\eta_1^2 \quad (6.2.1)$$

The unit vector along this curve is

$$\vec{t} = \frac{1}{\sqrt{1 + T^2}} (\vec{t}_e + T\vec{j}_e) \quad (6.2.2)$$

where

$$T = 2(P\xi + Q\eta_1) \quad (6.2.3)$$

The velocity due to the vortex is

$$\vec{V}_T = \int_C \frac{\vec{\xi} \times \vec{r}}{r^3} \mu ds \quad (6.2.4)$$

where μ is the edge value of the equivalent dipole strength. Arc length along the curve is related to distance in the tangent plane by

$$ds = \sqrt{1 + T^2} d\xi \quad (6.2.5)$$

Thus with r expressed in panel coordinates (Figure 1)

$$\begin{aligned} (\vec{\xi} \times \vec{r}) ds = & \left\{ \begin{bmatrix} 0 & -T(y - \eta_1) \\ z & +T(x - \xi) + \zeta \end{bmatrix} \begin{bmatrix} \vec{i}_e \\ \vec{j}_e \end{bmatrix} \right. \\ & \left. [(y - \eta_1) + 0] \vec{k}_e \right\} d\xi \end{aligned} \quad (6.2.6)$$

where the terms in the first column of (6.2.6) are first order, and those in the second column are second order. This expression is exact except for the approximation $\zeta = \zeta_2$.

As shown in reference 7 a three term expansion of $1/r^3$ is

$$\frac{1}{r^3} = \frac{1}{r_f^3} [1 + 3c_1 + 3(c_1^2 + c_2)] \quad (6.2.7)$$

where

$$\begin{aligned} c_1 &= \frac{z\zeta_2}{r_f^2} \\ c_2 &= \frac{3}{2} c_1^2 - \frac{1}{2} \frac{\zeta_2^2}{r_f^2} \end{aligned} \quad (6.2.8)$$

Along the N-line the equivalent dipole strength varies linearly

$$\mu = B(h + \xi) \quad (6.2.9)$$

where h is the total arc length along the N-line up to the η -axis of panel coordinates (see section 9.2 of reference 2), and B is the unknown value of

vorticity that is determined from the Kutta condition. The fundamental flow is obtained by setting B equal to unity in (6.2.9). Multiplying the above expansions gives the components of the vortex velocity as follows

$$\begin{aligned}
 V_{rx} &= \int_{\xi_1}^{\xi_2} \frac{1}{r_f^3} \left\{ 0 - [T(y - \eta_1)h] - [T(y - \eta_1)(3c_1h + \xi)] \right\} d\xi \\
 V_{ry} &= \int_{\xi_1}^{\xi_2} \frac{1}{r_f^3} \left\{ -zh + [-z(3c_1h + \xi) + h(T(x - \xi) + \xi_2)] \right. \\
 &\quad \left. + [-z(3(c_1^2 + c_2)h + 3c_1\xi) + (3c_1h + \xi)(T(x - \xi) + \xi_2)] \right\} d\xi \\
 V_{rz} &= (y - \eta_1) \int_{\xi_1}^{\xi_2} \frac{1}{r_f^3} \left\{ h + [3c_1h + \xi] + [3(c_1^2 + c_2)h + 3c_1\xi] \right\} d\xi
 \end{aligned} \tag{6.2.10}$$

6.3 Formulas for the Edge-Vortex Influence

The integrals in (6.2.10) have the form

$$J_{mn} = \int_{\xi_1}^{\xi_2} \frac{\xi_n^m}{r_f^n} d\xi \tag{6.3.1}$$

Once the J_{0n} and J_{1n} have been calculated the others are calculated from the recursion formulas

$$J_{mn} = J_{(m-2)(n-2)} + 2xJ_{(m-1)n} - p^2J_{(m-2)n} \tag{6.3.2}$$

where

$$p^2 = x^2 + (y - \eta_1)^2 + z^2 \tag{6.3.3}$$

The required J_{0n} and J_{1n} are

$$J_{01} = \log \frac{r_1 + r_2 + d_{12}}{r_1 + r_2 - d_{12}} = -L^{(12)} \quad (\text{eq. (7.7.3) reference 1})$$

$$J_{11} = r_2 - r_1 + xJ_{01}$$

$$J_{03} = \frac{1}{q^2} \left[\frac{\xi_2 - x}{r_2} - \frac{\xi_1 - x}{r_1} \right] \quad (6.3.4)$$

$$J_{13} = \frac{1}{r_1} - \frac{1}{r_2} + xJ_{03}$$

$$J_{05} = \frac{1}{3q^2} \left[\frac{\xi_2 - x}{r_2^3} - \frac{\xi_1 - x}{r_1^3} + 2J_{03} \right]$$

$$J_{15} = -\frac{1}{3} \left(\frac{1}{r_2^3} - \frac{1}{r_1^3} \right) + xJ_{05}$$

$$J_{07} = \frac{1}{5q^2} \left[\frac{\xi_2 - x}{r_2^5} - \frac{\xi_1 - x}{r_1^5} + 4J_{05} \right]$$

$$J_{17} = \frac{1}{5} \left(\frac{1}{r_1^5} - \frac{1}{r_2^5} \right) + xJ_{07}$$

where

$$q^2 = (y - \eta_1)^2 + z^2 \quad (6.3.5)$$

and where r_1 and r_2 are, respectively, distances of the point (x, y, z) from the ends of the interval, i.e.,

$$r_k^2 = (x - \xi_k)^2 + (y - \eta_1)^2 + z^2 \quad (6.3.6)$$

which is the same definition used in references 1 and 2.

In terms of certain auxiliary functions F_n the velocity components of (6.2.10) are

$$V_{rx} = -(y - \eta_1)[hF_1 + F_5]$$

$$V_{ry} = -zhJ_{03} + [-zF_2 + hF_3] - z[3hF_4 + F_6] + F_7 \quad (6.3.7)$$

$$V_{rz} = (y - \eta_1)[hJ_{03} + F_2 + 3hF_4 + F_6]$$

The auxiliary functions for on-body panels are:

$$F_1 = 2PJ_{13} + 2Qn_1J_{03}$$

$$F_2 = 3zh[PJ_{25} + 2Qn_1J_{15} + Rn_1^2J_{05}] + \{J_{13}\}$$

$$F_3 = 2PxJ_{13} + 2Qn_1xJ_{03} - PJ_{23} + Rn_1^2J_{03}$$

$$F_4 = \frac{5}{2} z^2 Q_7 - \frac{1}{2} Q_5$$

$$Q_j = [P^2J_{4j} + 4PQn_1J_{3j} + (2PR + 4Q^2)n_1^2J_{2j} + 4QRn_1^3J_{1j} + R^2n_1^4J_{0j}] \quad (6.3.8)$$

$$F_5 = 6zh[P^2J_{35} + 3PQn_1J_{25} + PRn_1^2J_{15} + 4QRn_1^3J_{05}] + \{2PJ_{23} + 2Qn_1J_{13}\}$$

$$F_6 = \{3z[PJ_{35} + 2Qn_1J_{25} + Rn_1^2J_{15}]\}$$

$$F_7 = 3zh[-P^2J_{45} + (2P^2x - 2PQn_1)J_{35} + 6PQxn_1J_{25} + (4Q^2xn_1^2 + 2PRxn_1^2 + 2QRn_1^3)J_{15} + (2QRxn_1^3 + R^2n_1^4)J_{05}] + \{-PJ_{33} + 2PxJ_{23} + (2Qxn_1 + Rn_1^2)J_{13}\}$$

The formulas for wake panels are obtained from (6.3.8) by deleting all terms in {} and replacing h by L (total) (section 9.2.2, reference 2).

For the semi-infinite last wake additional changes are made to the formulas (6.3.4) for the J_{mn} corresponding to

$$\xi_2 \rightarrow \infty \quad r_2 \rightarrow \infty \quad \xi_2/r_2 \rightarrow 1 \quad (6.3.9)$$

Furthermore P and Q are set equal to zero.

6.4 Far-Field Formulas

Originally it had been thought that edge vortices would be required only along physical edges of a lifting body, such as wing tips. In such a case no approximate far-field formulas would be needed, because the total number of edge-vortex influences would be a small fraction of the panel source influences.

However, numerical experimentation showed that for good accuracy edge vortices are required along all streamwise panel edges, i.e. along all N-lines of a lifting body. Thus the total number of edge-vortex influences is substantially twice the number of source influences, and simple far-field formulas are needed to reduce the computing time. These are used along interior edges. The notation is the same as in section 6.3, which refers to the first edge of a panel.

Compute

$$r_F^2 = \left[x - \left(\frac{\xi_1 + \xi_2}{2} \right) \right]^2 + [y - \eta_1]^2 + z^2 \quad (6.4.1)$$

If $(\xi_2 - \xi_1)^2 / r_F^2 < 0.001$, use

$$\begin{aligned} V_{rx} &= -(y - \eta_1) T_0 I \\ V_{ry} &= [-z + T_0 \left(x - \frac{\xi_1 + \xi_2}{2} \right) + \epsilon_0] I \\ V_{rz} &= (y - \eta_1) I \end{aligned} \quad (6.4.2)$$

where

$$\begin{aligned} I &= \frac{\xi_2 - \xi_1}{r_F^3} \left(h + \frac{\xi_1 + \xi_2}{2} \right) \\ T_0 &= 2 \left[P \frac{\xi_1 + \xi_2}{2} + Q \eta_1 \right] \\ \epsilon_0 &= P \left(\frac{\xi_1 + \xi_2}{2} \right)^2 + 2Q \eta_1 \left(\frac{\xi_1 + \xi_2}{2} \right) + R \eta_1^2 \end{aligned} \quad (6.4.3)$$

For the second N-line the obvious quantities are replaced by the corresponding ones. The above equations replace the elaborate formulas of the previous section.

7.0 MODIFICATION OF THE GLOBAL VORTICITY ALGORITHM

7.1 Considerations of Continuity and Accuracy

In general the singularities are discontinuous from one panel to the next over the surface of the body, i.e., across the interior panel edges. In a consistent method these discontinuities are higher order in some sense, but it seems intuitively desirable to reduce or eliminate them. However, the very useful method of reference 1 did not appear to suffer very much from their presence. The discontinuity in source strength is an unavoidable consequence of the basic method of solution as described in reference 2, section 8.0. In any event experience indicates that inaccuracies due to source discontinuities are relatively unimportant. It is the problem of dipole discontinuity that is addressed here.

If the lifting effects are accounted for by means of dipole distributions on the panels, e.g., reference 1, then a discontinuity of dipole strength yields a concentrated line vortex along the edge of a panel whose effects presumably are almost cancelled by the corresponding edge vortex of the adjacent panel. Thus the possible inaccuracies are due to presence of weak line-vortex singularities lying in the surface where clearly no such singularity exists. In the present method, however, the lifting effects are accounted for by means of vorticity distributions on the panels which are derived from an equivalent dipole distribution. If this last is discontinuous across interior panel edges, there will be no line vortex. Instead the computed velocity field will be slightly nonpotential. It is not obvious which of the above two types of error is larger or if either is particularly serious. Nevertheless, it seemed useful to try to minimize the effect of this source of error.

There are two distinct phenomena that cause the equivalent dipole distribution to be discontinuous. The first is geometric. In general, the edges of adjacent panels are not exactly coincident, and thus cancellation of edge singularities cannot be exact. This situation is unavoidable in the present method and will not be considered further. Attention has been directed towards the second cause of discontinuity, namely nonagreement of the equivalent dipole distributions of adjacent panels along their common edge. There are two types of interior edges — spanwise and streamwise, the latter of which lie along the

N-lines. Section 7.2 addresses the question of obtaining continuity of the equivalent dipole distributions across spanwise edges by suitably modifying the spanwise dipole variation and thus the chordwise vorticity variation. Exact continuity can be obtained in the absence of geometric discontinuity. Section 7.3 discusses a modification of the spanwise vorticity variation that apparently produces an improvement but not exact continuity.

7.2 Modification of the Chordwise Vorticity on a Panel

The basic analysis has been carried out in reference 1 for the flat panel case, and it applies to the present method as well under the assumption of coincident panel edges. As stated in section 7.3.4 of reference 1, the dipole strength is in general discontinuous between two adjacent panels of the same lifting strip unless a term quadratic in spanwise location is added to each panel distribution. The form of this term is

$$c\Delta B (\eta - \eta_1)(\eta - \eta_3) \quad (7.2.1)$$

where η is the spanwise panel coordinate, η_1 and η_3 are the locations of the parallel sides, ΔB is the change in vorticity strength across the span of the panel (zero if a piecewise constant B variation is used) and c is a constant to be adjusted for continuity. As shown in section 7.3.4 of reference 1, continuity between panels i and $i + 1$ of a strip is obtained if

$$w^{(i)} [c^{(i)} w^{(i)} + m_{32}^{(i)}] = w^{(i+1)} [c^{(i+1)} w^{(i+1)} + m_{41}^{(i+1)}] \quad (7.2.2)$$

where w is panel width (usually the same for all panels of a strip), m_{32} is the slope of the upper panel edge and m_{41} the slope of the lower panel edge. Equation (7.2.2) is solved for successive values of $c^{(i)}$ beginning with

$$c^{(1)} = 0 \quad (7.2.3)$$

and proceeding over all on-body panels of the strip. The choice (7.2.3) is arbitrary and expresses the fact that equations (7.2.2) have a nonunique solution, once the values of c for on-body panels have been calculated. The wake values are given by the procedure of section 7.9 of reference 1.

7.3 Modification of the Spanwise Fitting Procedure

In the standard option of the present method the variation of the equivalent dipole strength along an N-line is Bs where B is a constant and s is arc length measured around the contour from the trailing edge, e.g., equation (7.3.1) of reference 1 or (138) of reference 2. Thus B denotes vorticity strength normal to an N-line, i.e., bound vorticity. The total circulation around the section defined by the N-line is BL (total), where L (total) is the total arc length around the section from lower trailing edge to upper trailing edge.

The spanwise fitting option described in section 7.11 of reference 1 uses a piecewise constant or a piecewise linear fit to the values of B . Only the linear fit is permitted in the higher-order method of reference 2. However, it is clear from equation (7.9.1) of reference 1 that the equivalent dipole distribution in the wake depends on values of BL (total) rather than B . This is clear also on physical grounds since the strength of the trailing wake vorticity equals the spanwise derivative of the bound circulation, which is BL (total). Accordingly a fit in terms of B can lead to extraneous wake vorticity that does not necessarily vanish in the limit of small strip width. Since the method of reference 1 has given many good results, clearly the above effect is not important in many cases. Nevertheless it seemed useful to eliminate this possible source of inaccuracy, and the spanwise fits have been modified to accommodate BL (total) rather than B . This change also has the effect of reducing the discontinuity of the equivalent dipole distribution across N-lines and thus the magnitude of the required edge vorticities.

8.0 THE USE OF AN EXTRAPOLATED KUTTA CONDITION

The present method and its first-order predecessor both use an equal-pressure Kutta condition, in which the squares of the velocities on the upper and lower surfaces of the trailing edge are required to be equal. In the first-order method of reference 1 the velocities used are those at the control points nearest the trailing edge on the upper and lower surfaces of the wing. Thus in effect the Kutta condition is applied a finite distance, i.e., half a panel length, forward of the trailing edge. This approximation is sufficient for conventional airfoils where the difference between the upper- and lower-surface pressures a short distance ahead of the trailing edge is small. However, for supercritical airfoils pressure gradients near the trailing edge are large and even a short distance forward the difference between upper- and lower-surface pressures is substantial. Requiring these pressures to be equal at a location where they actually are quite different results in a considerable loss of lift. This situation was obscured for the first-order method by other inaccuracies that occur in cases of supercritical airfoils. However, the higher-order method handles such airfoils much more accurately and the use of the older form of the Kutta condition penalizes such a method unnecessarily.

The numerical implementation is quite simple. Using velocity components at the two control points nearest the trailing edge on the upper and lower surfaces, linear extrapolation gives values of these components "at" the trailing edge. The sum of the squares of the upper- and lower-surface components are then equated in the usual way.

9.0 CALCULATED EXAMPLES

The formulas presented in this report have been thoroughly verified to establish that they are coded as they are written. The larger questions of the correctness and effectiveness of the approach and the appropriateness of the various orders of approximation cannot be answered exactly because of the lack of analytic solutions with which to compare. The effectiveness of the approach will be established by frequent use, which will gradually produce a qualitative feel for its accuracy. A small start has been made in this direction. Several cases have been run to illustrate various features of the method and to compare it with the first order method of reference 1.

The calculated examples are of two types. The first compares various options of the program to determine their relative importance and to establish tentatively the proper use of the method. The second-type illustrates the scope of the method by presenting results for realistic examples.

A series of cases was run with the edge vortex formulas of section 6.0 and the global vorticity feature of section 7.2 to establish the relative importance of spanwise and streamwise edge vortices on a panel. The body used for this study is the swept wing of Figure 2a. Calculations were performed with the first-order method of reference 1 and with the present method suppressing both curvature and source-derivative effects. Differences between the two cases are due solely to edge-vortex effects. If the edge-vortex terms of section 6.0 are used along all N-lines the present method and the first-order method have the same trailing vortices. If either the piecewise-constant spanwise vorticity option is used or the piecewise-linear spanwise vorticity option is used with the global vorticity feature of section 7.2, then neither method has vortices along spanwise panel edges. If the features of both the last two sentences are used, then the two programs should give identical answers. This was verified explicitly. If the N-line edge vortices are retained but the piecewise-linear spanwise vorticity option is used without the feature of section 7.2, the first-order method has vortices along spanwise panel edges while the present method does not. A comparison of the calculated results then indicates the importance of the spanwise edge vortices. The two span-load distributions are essentially identical as are the pressure distributions except for the peak velocities, which are slightly different. It is concluded that the use of the

feature of section 7.2 is desirable because it offers some improvement, but that the level of discrepancy does not warrant special edge-vortex formulas for spanwise panel edges for curved-panel cases where exact cancellation of these vortices cannot be attained.

The study of the previous paragraph was continued by using the present method with an edge vortex on the tip N-line only and comparing its results to those obtained using edge-vortices on all N-lines. To minimize the strengths of the interior edge vortices, the piecewise-linear spanwise vorticity option was used. Figure 3 compares the two spanwise distributions of section lift coefficients. It can be seen that the neglect of trailing vortices on the interior N-lines yields a somewhat wiggly lift distribution of reduced level. Accordingly, it was decided to include these vortices in all future calculations.

As described in section 8.0, the Kutta condition in the first-order method has been applied by requiring equal pressures at the control points nearest the trailing edge on the upper and lower surfaces, i.e., the equal-pressure condition is applied a finite distance forward of the trailing edge. On supercritical wings, for which pressure gradients are large in the trailing edge regions, this can lead to an underprediction of lift. As a remedy, a new form of the Kutta condition has been developed in which upper- and lower-surface pressures are separately extrapolated to the trailing edge, and these extrapolated values are set equal. Sample results are shown in Figure 4 for the supercritical wing whose planform is shown in Figure 2b and whose airfoil section is as given in Figure 4. As is evident in Figure 4a, the requirement of pressure equality forward of the trailing edge pulls the pressure curve inside the more correct one. The resulting loss of lift is more easily seen in the spanwise distribution of Figure 4b and in the values of total lift. Thus the extrapolated Kutta condition is used exclusively in the present method.

To compare the present method with the first-order method of reference 1, calculations were performed for the conventional wing whose planform is shown in Figure 2a and whose airfoil section is given in Figure 5 and also for the wing-fuselage shown in Figure 6. Results for the clean wing are shown in Figure 5. As expected from two-dimensional experience, there is not a great deal of difference between the two methods for such a simple geometry. Nevertheless, some change in pressure distribution is evident in Figure 5a. The most significant difference is in the spanwise lift distribution shown in Figure 5b

where it is seen that the higher-order method gives higher tip loadings and lower root loadings.

Despite its greater geometrical complexity, the results for the wing-fuselage are not very different for the two programs, as shown in Figure 7. The higher-order method yields a smoother spanwise variation of section lift coefficient.

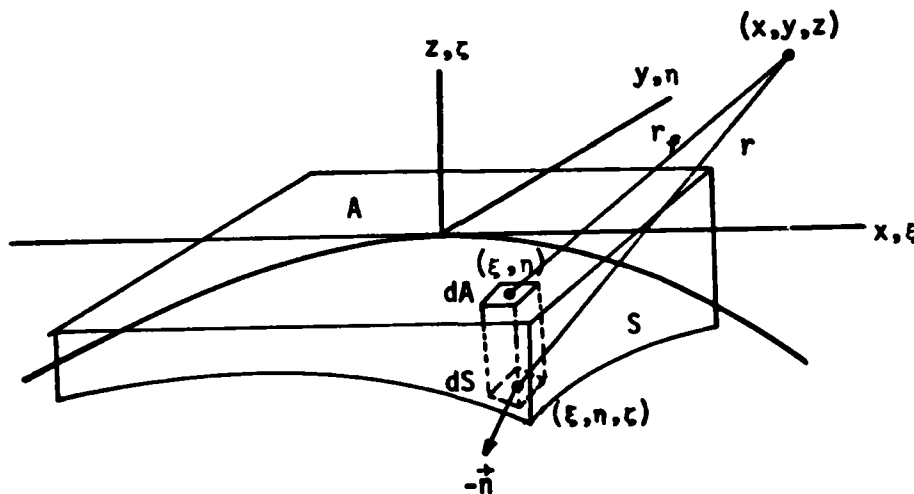
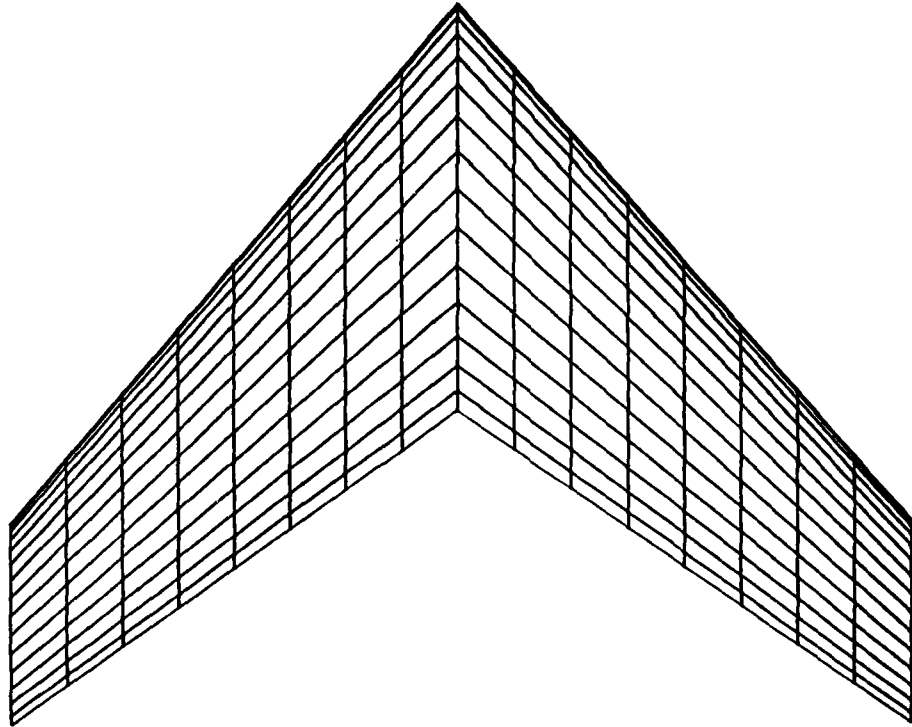
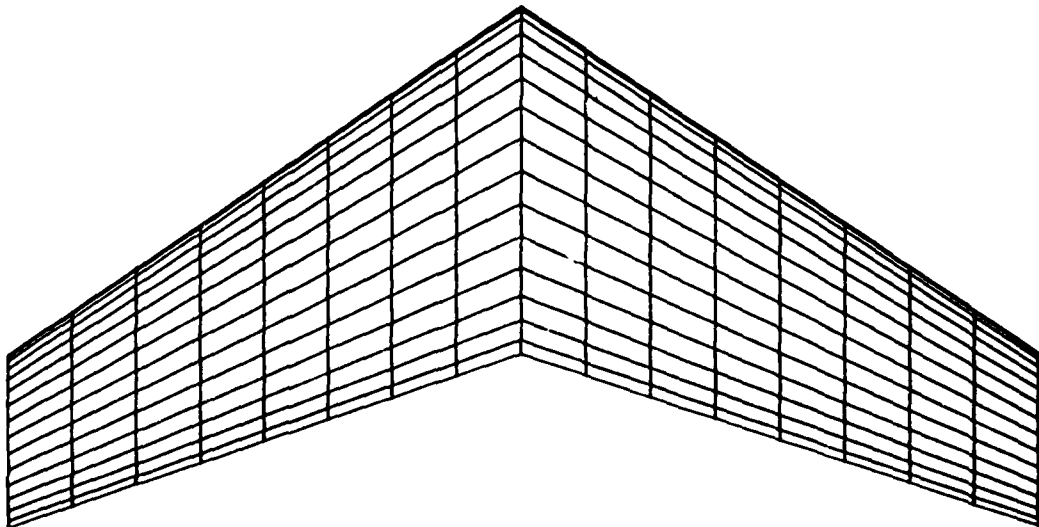


Figure 1. A general curved surface panel and its projection in the tangent plane.



(a) The conventional wing.



(b) The supercritical wing

Figure 2. Planforms and panel distributions for two wings.

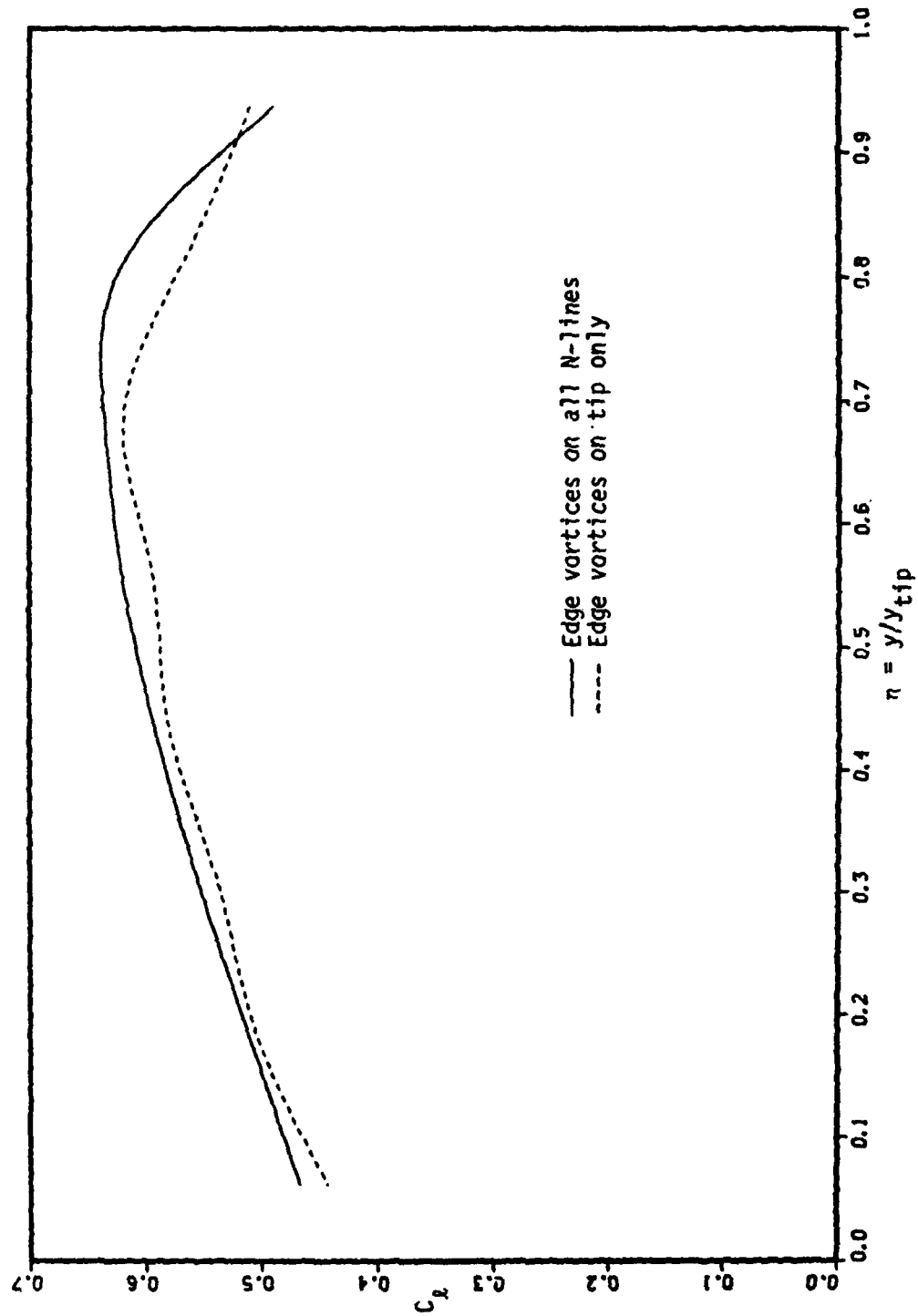
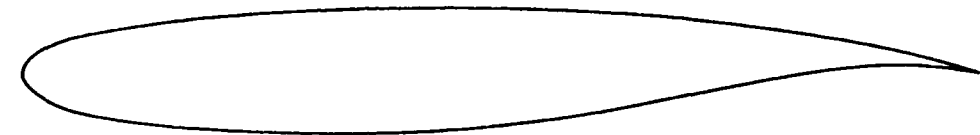
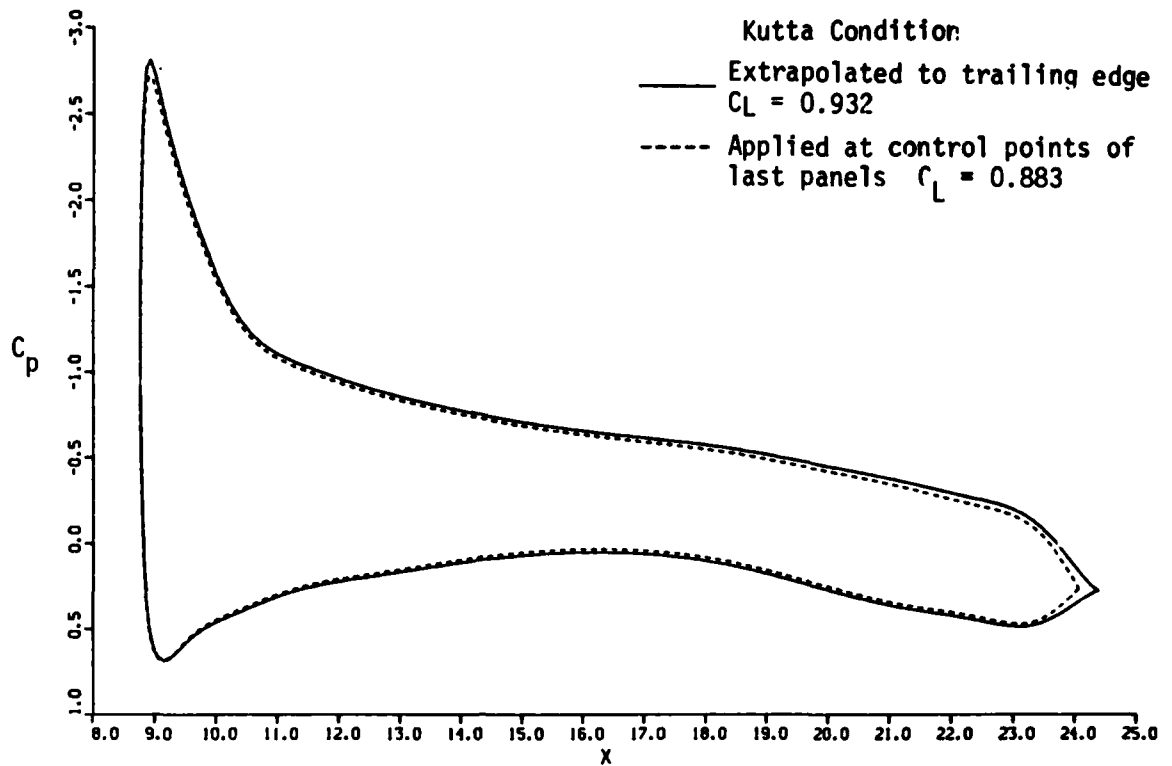
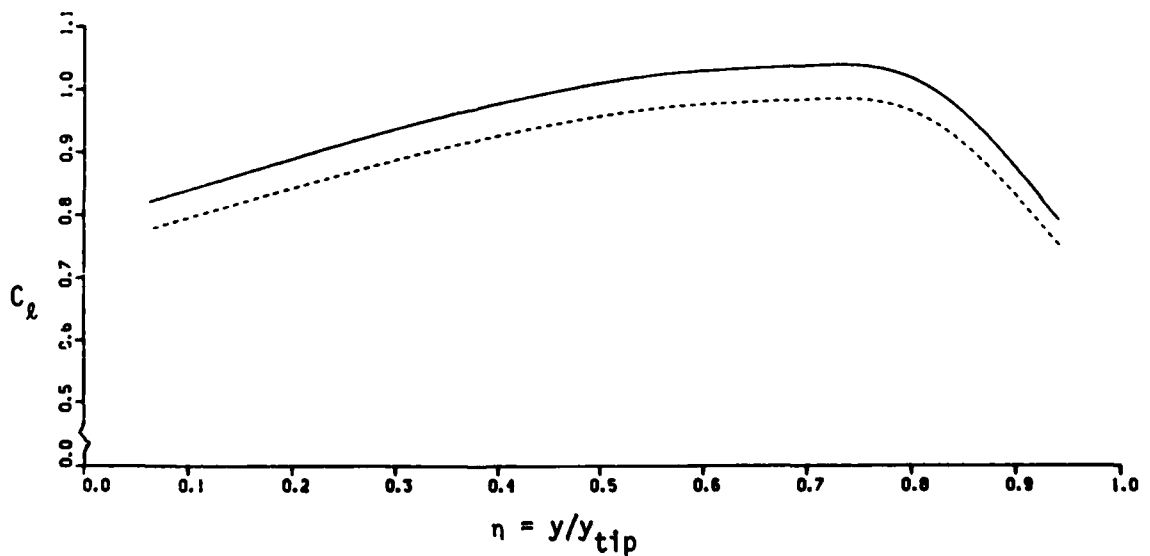


Figure 3. Spanwise variation of section lift coefficient for the conventional wing using two different options for the trailing vorticity.

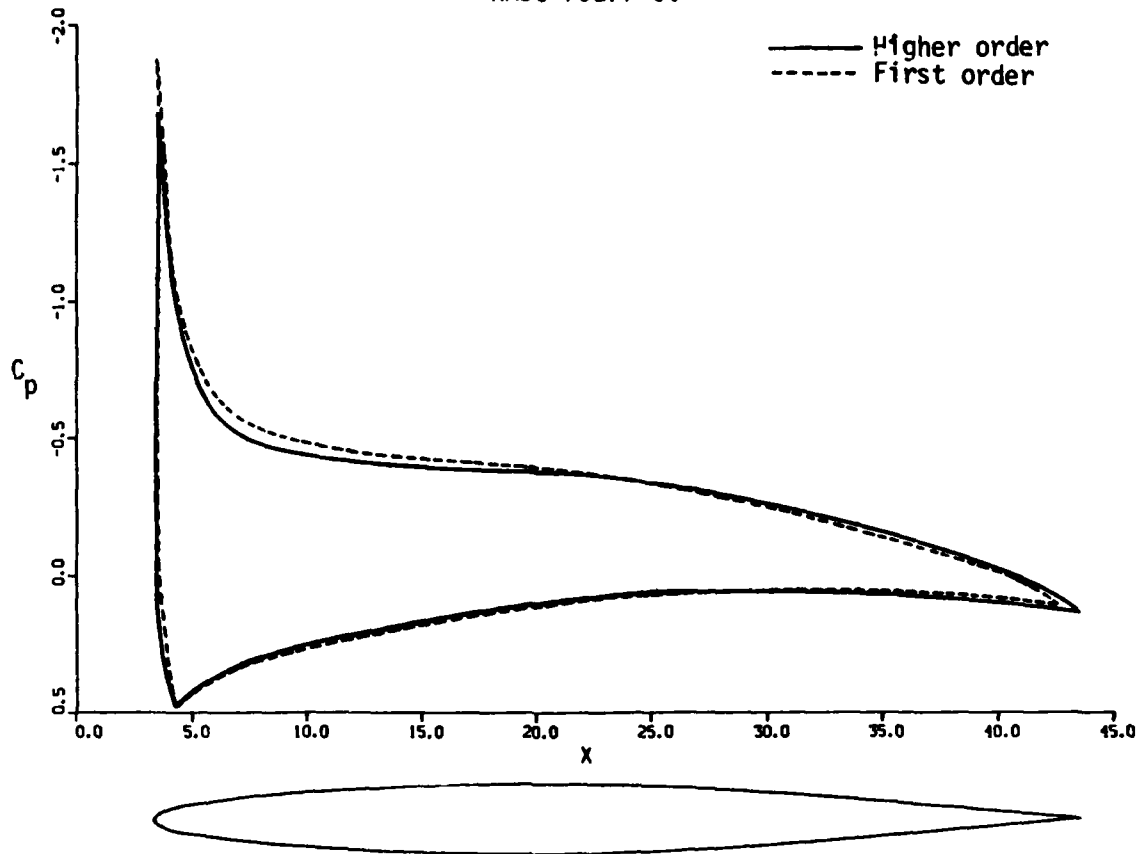


(a) Chordwise pressure distributions at mid-semi-span

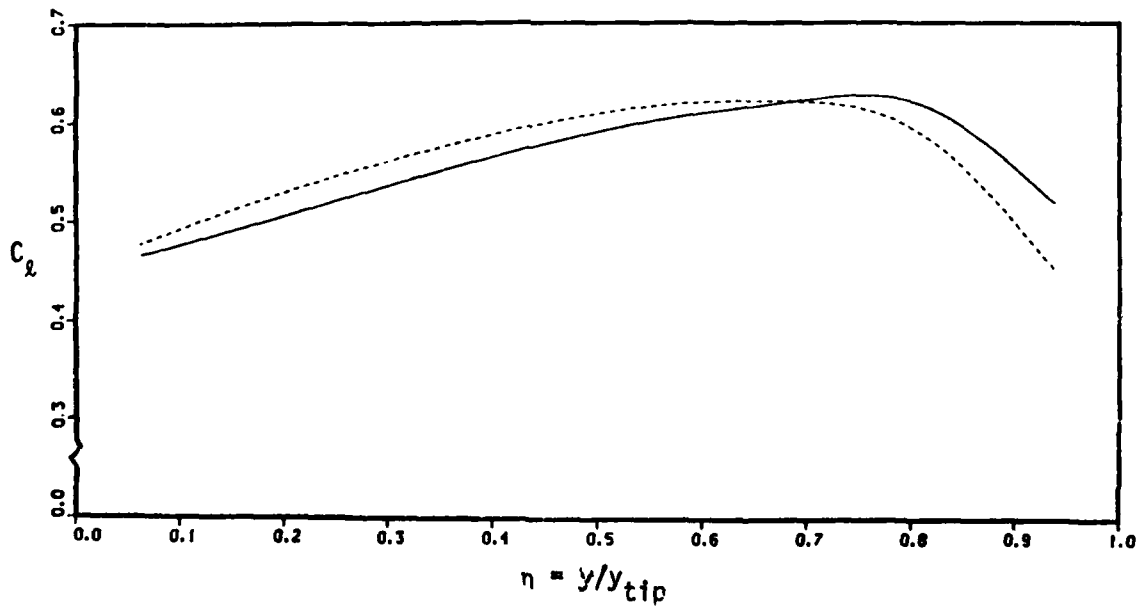


(b) Spanwise variations of section lift coefficient.

Figure 4. Calculated results for the supercritical wing with and without the extrapolated Kutta condition.



(a) Chordwise pressure distributions near the root.



(b) Spanwise variation of section lift coefficient.

Figure 5. Calculated results for a conventional wing.

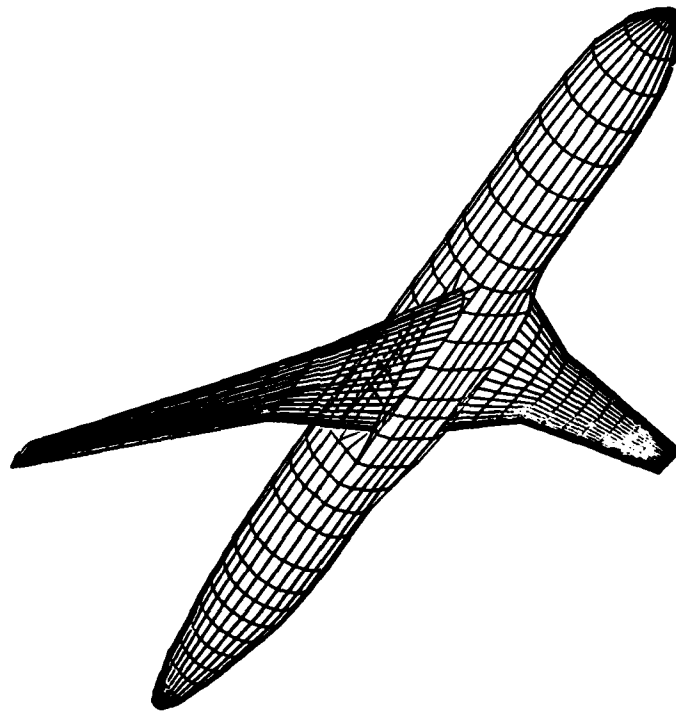
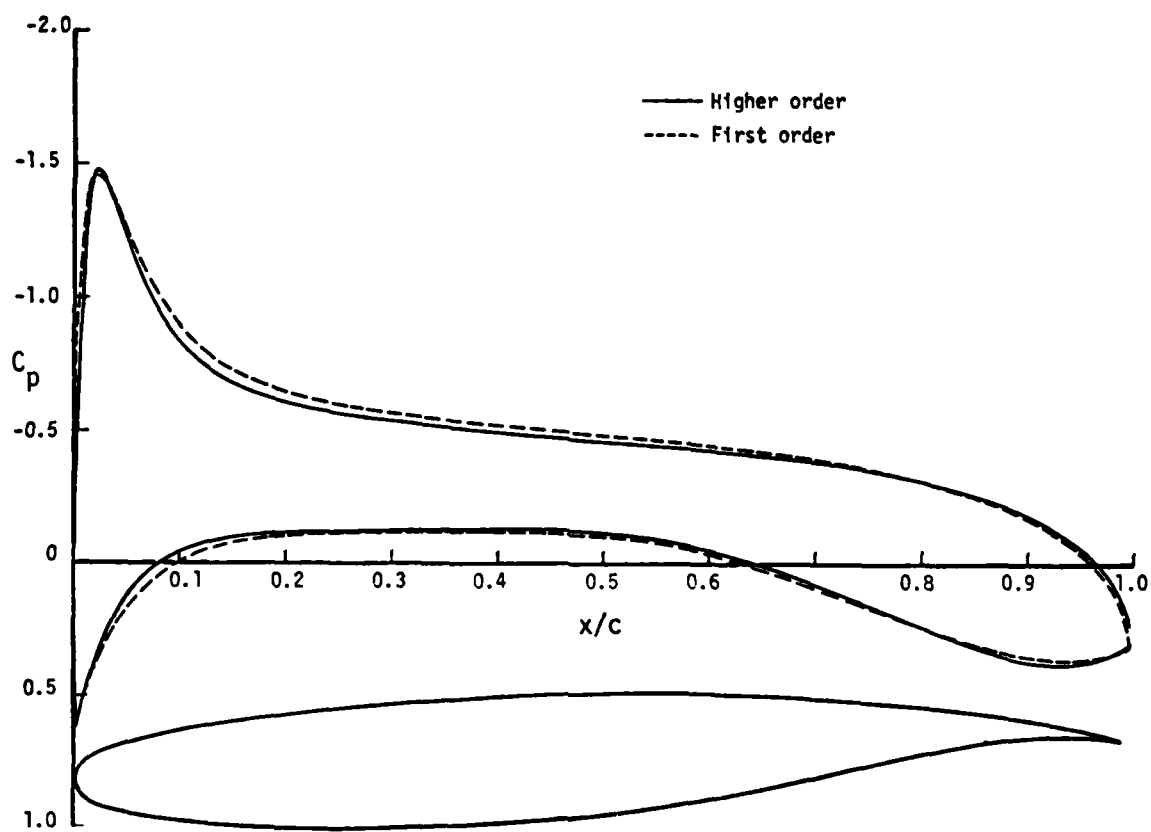
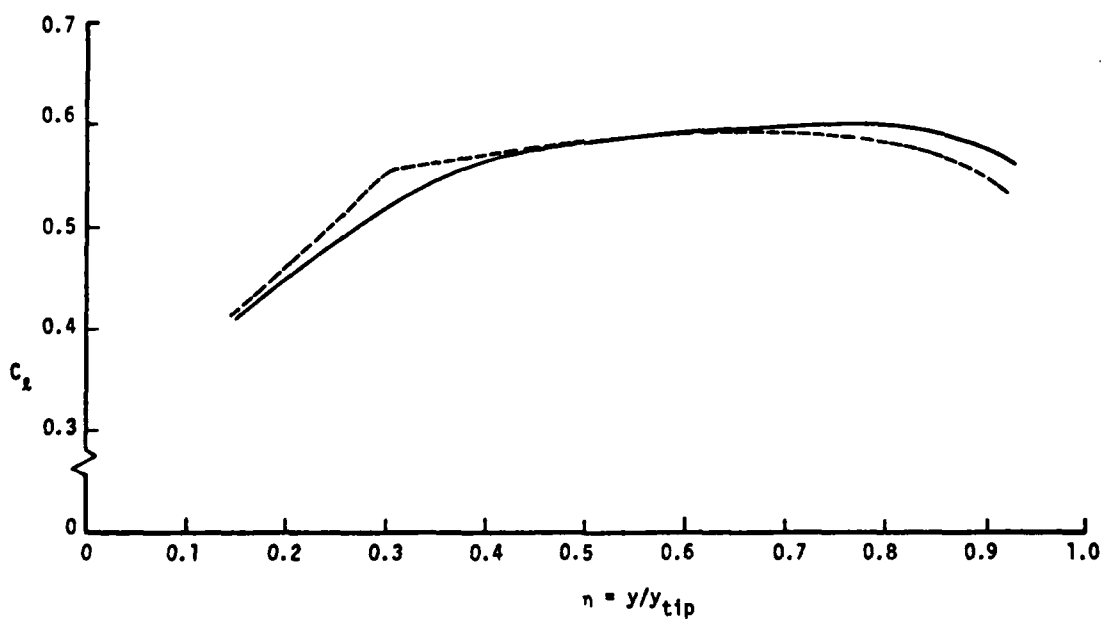


Figure 6. A wing-fuselage geometry showing the panel distribution.



(a) Chordwise pressure distributions near the root



(b) Spanwise variation of section lift coefficient

Figure 7. Calculated results for a wing-fuselage combination.

10.0 REFERENCES

1. Hess, J.L.: Calculation of Potential Flow about Arbitrary Three-Dimensional Lifting Bodies. McDonnell Douglas Report No. MDC J5679-01, October 1972.
2. Hess, J.L.: A Higher-Order Panel Method for Three-Dimensional Potential Flow. Report No. NADC 77166-30, June 1979.
3. Hess, J.L.: Status of a Higher-Order Panel Method for Nonlifting Potential Flow. Report No. NADC-76118-30, August 1977.
4. McComb, J.G., Parsons, S.V., and Wilson, J.A.: Exhaust System Performance Improvement for a Long-Duct Nacelle Installation for the DC-10. AIAA Paper No. 80-1195, June 1980.
5. Hess, J.L.: Higher-Order Numerical Solution of the Integral Equation of the Two-Dimensional Neumann Problem. Computer Methods in Applied Mechanics and Engineering, Vol. 2, No. 1, February 1973.
6. Semple, W.G.: A Note on the Relationship of the Influences of Sources and Vortices in Incompressible and Linearized Compressible Flow. British Aircraft Corp. (Military Aircraft Division) Report No. Ae/A/541, October 1977.
7. Hess, J.L.: Consistent Velocity and Potential Expansions for Higher-Order Singularity Methods. McDonnell Douglas Report No. MDC J6911, June 1975.
8. Peters, G.J.: Interactive Computer Graphics Application of the Parametric Bicubic Surface to Engineering Design Problems. Computer Aided Geometric Design (Eds.: Barnhill, R.E. and Riesenfeld, R.F.) Academic Press, New York, 1974.
9. Struik, D.J.: Differential Geometry. Addison-Wesley, Cambridge, 1950.

APPENDIX A

A SURFACE GEOMETRY FITTING PROCEDURE BASED ON BICUBIC SPLINES

The original least-square fitting procedure for P, Q and R, as described in section 7.2 of reference 2, proved satisfactory for many geometries. However, it broke down for large panel aspect ratios, as for example occur near wing leading edges. Several modifications were attempted, including weighted least squares and double-precision arithmetic, but none proved satisfactory for every application. Accordingly, it was decided to try a completely new geometric procedure to replace that of section 7.0 of reference 2. This approach effectively decouples the geometric calculation from the fluid dynamic one, and it has proved more accurate and versatile than any of its predecessors.

Very elaborate geometry fitting procedures based on parametric bicubic splines have been developed at Douglas Aircraft Company over many years. A description of this technique is beyond the scope of the present report. A survey is contained in reference 8. In the present application the method is considered a "black box," although several minor changes had to be made.

The points defining the body are input in the usual way. Each panel is fitted by a bicubic surface in terms of two parameters u and v that vary from 0 to 1 over the panel. (The panel is the unit square in parameter space.) This permits the well-known procedures of reference 9 to be used as follows.

Let a point (x,y,z) of the panel be represented as a vector

$$\vec{x} = x\vec{i} + y\vec{j} + z\vec{k} \quad (A.1)$$

The parametric cubic fit then yields

$$\vec{x} = \vec{x}(u,v) \quad (A.2)$$

These expressions may be differentiated analytically to give

$$\vec{x}_u, \quad \vec{x}_v, \quad \vec{x}_{uu}, \quad \vec{x}_{uv}, \quad \vec{x}_{vv} \quad (A.3)$$

as functions of u and v . The vectors \vec{x}_u and \vec{x}_v are tangent to the curves $v = \text{constant}$ and $u = \text{constant}$, respectively, and thus lie in the surface although they are not perpendicular.

The point corresponding to $u = v = \frac{1}{2}$ is in the "center" of the panel in some sense. It is selected as the control point and origin of coordinates of the flat projected panel. The derivatives of (A.3) are evaluated there, and in all that follows \vec{x} and its derivatives are assumed to be those at $u = v = \frac{1}{2}$.

The unit normal vector to the panel, which is also the unit vector along the ζ axis of panel coordinates is

$$\vec{n} = \vec{k}_e = \pm \frac{\vec{x}_u \times \vec{x}_v}{|\vec{x}_u \times \vec{x}_v|} \quad (\text{A.4})$$

where the sign is selected to give an outward normal. The unit vector along the ξ axis of panel coordinates is taken tangent to the $v = \text{constant}$ curve which nearly parallels the N-lines,

$$\vec{t}_e = \frac{\vec{x}_u}{|\vec{x}_u|} \quad (\text{A.5})$$

Thus the unit vector along the η axis of panel coordinates is

$$\vec{j}_e = \vec{k}_e \times \vec{t}_e \quad (\text{A.6})$$

The components of the three unit vectors thus obtained are the transformation matrix. Compare equation (7.2.10) of reference 1.

Now define

$$h = u - \frac{1}{2}, \quad k = v - \frac{1}{2} \quad (\text{A.7})$$

and consider the Maclaurin series for ξ , η , and ζ in terms of h and k . They have the form

$$\begin{aligned} \xi &= Ah + Bk + (\text{second order}) \\ \eta &= Ch + Dk + (\text{second order}) \\ \zeta &= \frac{1}{2}(eh^2 + 2fhk + gk^2) + (\text{third order}) \end{aligned} \quad (\text{A.8})$$

There are no constant terms in (A.8), because the origin of panel coordinates corresponds to $h = k = 0$. Furthermore, since the $\xi\eta$ plane is tangent to the surface at the origin (\vec{k}_e is the normal vector), the series for ζ has no linear terms. Reference 9 gives the coefficients of equations (A.8) as

$$\begin{aligned}
 A &= \vec{x}_u \cdot \vec{t}_e & B &= \vec{x}_v \cdot \vec{t}_e \\
 C &= \vec{x}_u \cdot \vec{j}_e = 0 & D &= \vec{x}_v \cdot \vec{j}_e
 \end{aligned}
 \tag{A.9}$$

$$\begin{aligned}
 e &= \vec{x}_{uu} \cdot \vec{n} & f &= \vec{x}_{uv} \cdot \vec{n} & g &= \vec{x}_{vv} \cdot \vec{n}
 \end{aligned}
 \tag{A.10}$$

The first two of equations (A.8) may be inverted to give

$$\begin{aligned}
 h &= a\xi + b\eta + (\text{second order}) \\
 k &= c\xi + d\eta + (\text{second order})
 \end{aligned}
 \tag{A.11}$$

where

$$\begin{aligned}
 a &= \frac{D}{\Delta}, & b &= -\frac{B}{\Delta}, & c &= \frac{C}{\Delta}, & d &= \frac{A}{\Delta} \\
 \Delta &= AD - BC
 \end{aligned}
 \tag{A.12}$$

Equation (A.12) may be inserted into the third equation of (A.8) to give the desired form

$$\zeta = P\xi^2 + 2Q\xi\eta + R\eta^2
 \tag{A.13}$$

The result is

$$\begin{aligned}
 P &= \frac{1}{2}[ea^2 + 2fac + gc^2] \\
 Q &= \frac{1}{2}[eab + f(ad + bc) + gcd] \\
 R &= \frac{1}{2}[eb + 2fbd + gd^2]
 \end{aligned}
 \tag{A.14}$$

For generality c has been included in (A.14), but in the present application it is zero, which simplifies (A.14).

It remains to compute corner points in panel coordinates. The four input points bounding the panel are transformed into panel coordinates to obtain $(\xi_k^*, \eta_k^*, \zeta_k^*)$ $k = 1, 2, 3, 4$. They are projected into the plane by simply ignoring ζ_k^* . Next the side between points 1 and 2 is rotated to make $\eta_1 = \eta_2$. The midpoint and length of the side are, respectively,

$$\begin{aligned}\bar{\xi} &= \frac{1}{2}(\xi_1^* + \xi_2^*), & \bar{\eta} &= \frac{1}{2}(\eta_1^* + \eta_2^*) \\ d &= \sqrt{(\xi_1^* - \xi_2^*)^2 + (\eta_1^* - \eta_2^*)^2}\end{aligned}\tag{A.15}$$

Then the final corner point coordinates are

$$\begin{aligned}\eta_1 &= \eta_2 = \bar{\eta} \\ \xi_1 &= \bar{\xi} - \frac{d}{2} \\ \xi_2 &= \bar{\xi} + \frac{d}{2}\end{aligned}\tag{A.16}$$

A similar calculation is performed for the side between the points 3 and 4.

It should be noted that the underlying parametric cubic geometry routine uses the surrounding input points to generate the fit to a panel. The routine considers only points on the same section, and thus slightly different results can be obtained depending on how the body is sectioned. For fitting purposes the wake is considered a separate section, so that the routine does not try to fit around the trailing edge. On the semi-infinite last-wake panel the derivatives P and Q are set equal to zero, so that the panel has straight generators in the stream direction, but R , the spanwise second derivative, may be nonzero.

The parametric cubic procedure gives smooth fits even in extreme cases. By way of illustration the airfoil sections on a wing were defined by only four points, leading and trailing edges and upper and lower surface maximum-thickness points. Thickness was 20% at the root and mid-semispan and 10% at the tip. Results are shown in Figure A.1. Remarkably, the "diamond" section shapes have been fitted with reasonable, smooth curves, as opposed, for example, to what a parabolic fit would have done. It should be noticed that the leading edge is rounded and the trailing edge, from which the wake issues, is sharp as required. The fact that the trailing-edge angles are somewhat large is due to the absurdly inadequate point number.

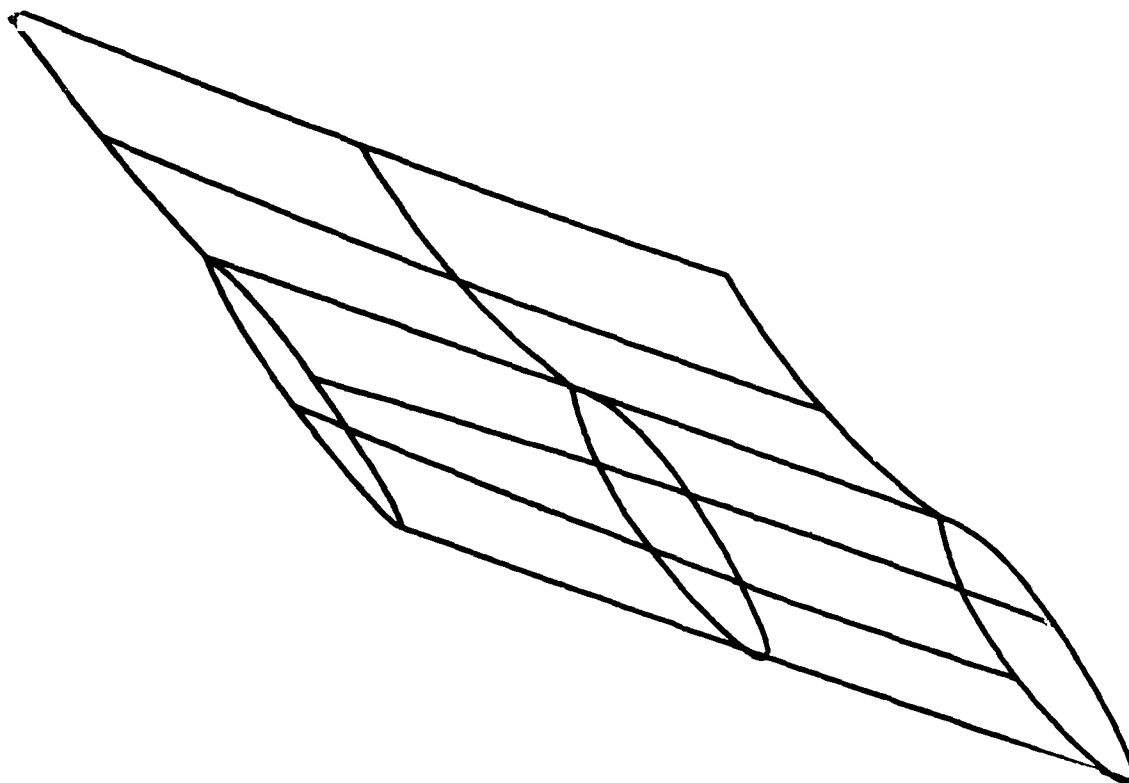


Figure A.1. Parametric cubic representation of a wing with four panels around each section.

Unclassified

SECURITY CLASSIFICATION OF THIS PAGE (When Data Entered)

REPORT DOCUMENTATION PAGE		READ INSTRUCTIONS BEFORE COMPLETING FORM												
1. REPORT NUMBER NADC-79277-60	2. GOVT ACCESSION NO. AD-A110 819	3. RECIPIENT'S CATALOG NUMBER												
4. TITLE (and Subtitle) An Improved Higher-Order Panel Method for Three-Dimensional Lifting Potential Flow		5. TYPE OF REPORT & PERIOD COVERED Final Report												
		6. PERFORMING ORG. REPORT NUMBER MDC J2162												
7. AUTHOR(s) John L. Hess		8. CONTRACT OR GRANT NUMBER(s) N62269-80-C-0228												
9. PERFORMING ORGANIZATION NAME AND ADDRESS Douglas Aircraft Company 3855 Lakewood Boulevard Long Beach, California 90846		10. PROGRAM ELEMENT, PROJECT, TASK AREA & WORK UNIT NUMBERS N62269-80-65-00495												
11. CONTROLLING OFFICE NAME AND ADDRESS Naval Air Development Center Warminster, PA 18904 (6052)		12. REPORT DATE December 1981												
		13. NUMBER OF PAGES												
14. MONITORING AGENCY NAME & ADDRESS (if different from Controlling Office)		15. SECURITY CLASS. (of this report) Unclassified												
		15a. DECLASSIFICATION/DOWNGRADING SCHEDULE												
16. DISTRIBUTION STATEMENT (of this Report) Approved for Public Release; Distribution Unlimited														
17. DISTRIBUTION STATEMENT (of the abstract entered in Block 20, if different from Report)														
18. SUPPLEMENTARY NOTES														
19. KEY WORDS (Continue on reverse side if necessary and identify by block number) <table border="0"> <tr> <td>Aerodynamics</td> <td>Higher Order</td> <td>Source Density</td> </tr> <tr> <td>Computer Program</td> <td>Numerical Analysis</td> <td>Surface Singularity</td> </tr> <tr> <td>Flow Field</td> <td>Panel Method</td> <td>Three-Dimensional Flow</td> </tr> <tr> <td>Fluid Dynamics</td> <td>Potential Flow</td> <td></td> </tr> </table>			Aerodynamics	Higher Order	Source Density	Computer Program	Numerical Analysis	Surface Singularity	Flow Field	Panel Method	Three-Dimensional Flow	Fluid Dynamics	Potential Flow	
Aerodynamics	Higher Order	Source Density												
Computer Program	Numerical Analysis	Surface Singularity												
Flow Field	Panel Method	Three-Dimensional Flow												
Fluid Dynamics	Potential Flow													
20. ABSTRACT (Continue on reverse side if necessary and identify by block number) <p>A previous report described a higher-order three-dimensional panel method that represents the body about which flow is to be computed by means of curved four-sided surface panels having linearly varying source and vorticity distributions. The method of accounting for lift was incomplete, and the main purpose of the present work was to remedy this defect. A number of other modifications to the method were also made to improve the efficiency and accuracy of the method.</p>														

DD FORM 1473
1 JAN 73

EDITION OF 1 NOV 65 IS OBSOLETE
S/N 0102-014-6601

Unclassified

SECURITY CLASSIFICATION OF THIS PAGE (When Data Entered)

Unclassified

SECURITY CLASSIFICATION OF THIS PAGE(When Data Entered)

The modifications documented here are: formulas for the edge-vortex influences, which previously had been neglected; new surface vorticity formulas that express its influences in terms of source influences; a modified global vorticity algorithm to improve continuity over the surface, and; an extrapolated Kutta condition.

Unclassified

SECURITY CLASSIFICATION OF THIS PAGE(When Data Entered)

DISTRIBUTION LIST

Report No. NADC-79277-60

AIRTASK No. A320320D/001A/1R023-02-000

	<u>No. of Copies</u>
NAVAIR (AIR-950D)	4
(2 for retention)	
(1 for AIR-320D)	
(1 for AIR-5301)	
NAVWPNCEN, China Lake, CA	1
NAVAIRPROPGEN, Trenton, NJ.	1
DTNSKDC, Bethesda, MD (Attn: Dr. H. Chaplin)	1
ONR, Arlington, VA (Attn: R. Whitehead).	1
NAVPGSCOL, Monterey, CA (Attn: M. Platzer)	1
NASA, Ames Research Center, Moffett Field, CA	2
(1 for D. Hickey)	
(1 for W. Deckert)	
NASA, Langley Research Center, Hampton, VA (Attn: R. Margason)	1
NASA, Lewis Research Center, Cleveland, OH.	1
Wright-Patterson AFB, Dayton, OH.	2
(1 for Flight Dynamics Lab)	
(1 for Aeronautical Systems Division)	
The Pentagon, Washington, DC (Attn: R. Siewert)	1
U.S. Army Aviation Systems Command, St. Louis, MO	1
U.S. Army Research Office, Durham, NC	1
DTIC, Alexandria, VA.	12
Boeing Company, Seattle, WA (Attn: E. Omar).	1
LTV Aerospace Corporation, Dallas, TX	2
(1 for T. Beatty)	
(1 for W. Simpkin)	
Rockwell International, Columbus, OH (Attn: W. Palmer)	1
General Dynamics Corporation, Ft. Worth, TX (Attn: W. Folley).	1
Nielson Engineering, Mountain View, CA (Attn: S. Spangler)	1
Univ. of Tennessee, Space Inst., Tullahoma, TN (Attn: W. Jacobs)	1
Lockheed-California Co., Burbank, CA (Attn: Y. Chin)	1
Northrop Corporation, Hawthorne, CA (Attn: P. Wooler).	1
Grumman Aerospace Corp., Bethpage, LI, NY (Attn: S. Kalamaris).	1
Royal Aeronautical Establishment, Bedford, England (Attn: A. Woodfield).	1
Fairchild-Republic, Corporation, Farmingdale, LI, NY.	1
Calspan, Buffalo, NY.	1
McDonnell Douglas Corp., St. Louis, MO (Attn: Dr. D. Kotansky)	1
V/STOL Consultant, Newport News, VA (Attn: R. Kuhn).	1
Georgia Inst., of Technology, Atlanta, GA (Attn: Dr. H. McMahon)	1
Penn State Univ., Univ. Park, PA (Attn: Prof. B. W. McCormick)	1

DA
FILM

3-